Size is a major determinant of dissociation and denaturation behaviour of reconstituted high-density lipoproteins

Elisabetta GIANAZZA*[1], Ivano EBERINI*, Cesare R. SIRTORI†, Guido FRANCESCHINI† and Laura CALABRESI†

*Gruppo di Studio per la Proteomica e la Struttura delle Proteine, Dipartimento di Scienze Farmacologiche, Università degli Studi di Milano, via G. Balzaretti 9, I-20133 Milano, Italy, and †Centro 'Enrica Grossi Paoletti', Dipartimento di Scienze, Farmacologiche, Università degli Studi di Milano, via G. Balzaretti 9, I-20133 Milano, Italy

Lipid-free apolipoprotein A-I (apoA-I) and A-I_{Milano} (A-I_M) were compared for their denaturation behaviour by running across transverse gradients of a chaotrope, urea, and of a ionic detergent, SDS. For both apo A-I and monomeric apoA-I_M in the presence of increasing concentrations of urea the transition from high to low mobility had a sigmoidal course, whereas for dimeric A-I_M/A-I_M a non-sigmoidal shape was observed. The co-operativity of the unfolding process was lower for dimeric A-I_M/A-I_M than for apoA-I or for monomeric apoA-I_M. A slightly higher susceptibility to denaturation was observed for dimeric A-I_M/A-I_M than for monomeric apoA-I_M. A similar behaviour of A-I_M/A-IM versus apoA-I_M was observed in CD experiments. Large- (12.7/12.5 nm) and small- (7.8 nm) sized reconstituted high-density lipoproteins (rHDL) containing either apoA-I or A-I_M/A-I_M were compared with respect to their protein–lipid dissociation behaviour by subjecting them to electrophoresis in the presence of urea, of SDS and of a non-ionic detergent, Nonidet P40. A higher susceptibility to dissociation of small-sized versus large-sized rHDL, regardless of the apolipoprotein component, was observed in all three instances. Our data demonstrate that the differential plasticity of the various classes of rHDL is a function of their size; the higher stability of 12.5/12.7 nm rHDL is likely connected to the higher number of protein–lipid and lipid–lipid interactions in larger as compared with smaller rHDL.

Key words: apolipoprotein A-I, non-ionic detergent, palmitoyl-oleoyl phosphatidylcholine, sodium dodecyl sulphate, urea + denaturant gradient gel electrophoresis.

INTRODUCTION

Apolipoprotein A-I (apoA-I) is the major protein constituent of human high-density lipoproteins (HDL) and is believed to be responsible for the antiatherogenic and antithrombogenic properties of HDL. ApoA-I is predicted to consist of a series of eight 22-amino-acid proline-punctuated class A amphipathic α-helices and two 11-amino-acid tandem repeats [1–3]. Two alternative theoretical models, based on amphipathic α-helices, have been presented for the tertiary structure of lipid-bound apoA-I. In the first – the 'picket-fence model' described by Phillips et al. [4] – the helices run antiparallel to one another (giving rise to intramolecular protein–protein interactions) and parallel to the lipid acyl chains. In the second – the 'belt model' described by Segrest et al. [5] – the helices run perpendicular to phospholipids (with intermolecular protein–protein interactions). Both models include two apoA-I and 160–161 L-α-palmitoyloleoyl phosphatidylcholine (POPC) molecules per particle. A novel hairpin folding of apoA-I monomer was recently proposed, with most helices perpendicular to the phospholipid acyl chains and a random head-to-tail and head-to-head arrangement of the two apoA-I molecules [6].

Upon interaction with phospholipids, apoA-I generates a number of discretely sized discoidal particles resembling nascent HDL, also known as reconstituted HDL (rHDL). These rHDL mimic most of the physiological properties of plasma HDL; they proved to be a valuable tool in identifying structural requirements for some HDL functions. Well-defined rHDL made with apoA-I and synthetic phosphatidylcholines, and with specific ratios between the components, have very reproducible sizes and compositions [7].

The apolipoprotein A-I_{Milano} (apoA-I_M) is a molecular variant of apoA-I characterized by an $Arg^{173} \rightarrow Cys$ substitution, leading to the formation of disulphide-linked dimers (A-I_M/A-I_M) [8]. While the structure of the lipid-free and lipid-bound apoA-I_M monomer only slightly differs from wild-type apoA-I [9], the introduction of an interchain disulphide bridge in the A-I_M/A-I_M homodimer remarkably alters the physico-chemical properties of apoA-I [10]. When compared with apoA-I, the lipid-free A-I_M/A-I_M displays a higher α-helical content and a more folded tertiary structure [10]. Upon interaction with phospholipids, A-I_M/A-I_M forms only two species of rHDL, with diameters of 7.8 and 12.5 nm, which contain one or two A-I_M/A-I_M molecules per particle respectively [11].

In the present investigations we compared the dissociation and the denaturation processes for rHDL containing either apoA-I or the dimeric form of A-I_{Milano} (A-I_M/A-I_M). Particles of different sizes and stoichiometry were produced with both proteins (Table 1). The evaluation of the relative stability of these rHDL, differing by just one parameter, allows us to assess its relevance. This may provide a better understanding of the nature and the strength of intermolecular interactions.

The analytical procedure we have used in our investigation was denaturant gradient gel electrophoresis (DGGE) [12]. When applied to ligand-free proteins, this technique allows correlating changes in electrophoretic mobility across a transverse gradient

Abbreviations used: apoA-I, apolipoprotein A-I; apoA-I_M, apolipoprotein A-I_{Milano}; rHDL, reconstituted high-density lipoproteins; 7.8 nm apoA-I rHDL, 12.7 nm apoA-I rHDL, 7.8 nm A-I_M/A-I_M rHDL and 12.5 nm A-I_M/A-I_M rHDL, reconstituted high-density lipoproteins, containing either apoA-I or A-IM dimer, 7.8, 12.5 or 12.7 nm in diameter; DGGE, denaturant gradient gel electrophoresis; NP40, Nonidet P40; PA, polyacrylamide; POPC, L-α-palmitoyloleoyl phosphatidylcholine.

[1] To whom correspondence should be addressed (e-mail elisabetta.gianazza@unimi.it).

Table 1 Characteristics of rHDL

Particle	Apo molecules per particle	Size (nm)	POPC/apolipoprotein Mass ratio (w/w)	POPC/apolipoprotein Molar ratio (mol/mol)
7.8 nm apoA-I rHDL	2 (apoA-I)	7.8	1.21 (±0.11):1	45 (±4):1
12.7 nm apoA-I rHDL	3 (apoA-I)	12.7	4.02 (±0.03):1	148 (±1):1
7.8 nm A-I_M/A-I_M rHDL	2 (1 A-I_M/A-I_M)	7.8	1.04 (±0.05):1	76 (±4):1
12.5 nm A-I_M/A-I_M rHDL	4 (2 A-I_M/A-I_M)	12.5	2.05 (±0.11):1	151 (±8):1

of a denaturing agent with the varying size of the sample protein. In fact, the hydrodynamic volume of proteins depends on their folded or unfolded and associated or dissociated status. For readers unfamiliar with the technique, a brief summary on the interpretation of results from DGGE experiments is given in the Materials and methods section. Approaches to data treatment were first discussed in [12,13]; a comprehensive review may be found in [14].

The equilibria $A_n \leftrightarrow nA$ or $A_nB_m \leftrightarrow nA + mB$ for dissociation, and $A_{folded} \leftrightarrow A_{unfolded}$ for denaturation, are driven to the left mostly by enthalpic factors and to the right by entropic factors. Accordingly, holoproteins are usually more stable against denaturation than their apo counterparts (as with transferrin [15], ovotransferrin [16], α-lactoglobulin [17] and carbonic anhydrase [18]).

We have already studied the behaviour of self-aggregating lipid-free apoA-I in the presence of increasing concentrations of urea: in DGGE a series of parallel transitions was observed from folded multimers to unfolded monomer [19]. With the present investigation we aimed to characterize the behaviour of rHDL, analysing lipid–lipid and lipid–protein interactions. With the use of urea, neutral [Nonidet P-40 (NP40)] and charged (SDS) detergents, we tried to differentiate lipid–protein dissociation from denaturation of the apolipoprotein components. DGGE has the advantage over spectroscopic techniques (CD and fluorescence quenching) of not hiding complexity. In fact spectroscopic techniques average optical properties over all molecular species in the sample. DGGE, by contrast, resolves all molecular species present at any given denaturant concentration.

MATERIALS AND METHODS

Reagents and supplies

A-I_M/A-I_M was expressed in the *Escherichia coli* and purified by conventional chromatographic procedures [10]. The A-I_M/A-I_M batch used in the present study contained ≈ 98 % of A-I_M/A-I_M, as determined by SDS/PAGE (results not shown). Normal apoA-I was purified from human blood plasma, as previously described [9]. Before use, freeze-dried A-I_M/A-I_M and apoA-I were dissolved in 20 mM phosphate buffer, pH 7.4, containing 6 M guanidinium chloride, and extensively dialysed against 10 mM Tris/HCl (pH 8.0)/150 mM NaCl/1 mM NaN_3/0.01 % EDTA. Protein concentration of the stock solutions was assayed by amino acid analysis, performed on a Beckman 6300 amino acid analyser after acidic hydrolysis of samples in 6 M HCl for 45 min at 155 °C. POPC was purchased from Sigma.

Preparation of reconstituted HDL

Discoidal rHDL containing A-I_M/A-I_M or apoA-I and POPC, with a diameter of 7.8 nm or 12.5–12.7 nm were prepared by the cholate dialysis technique [20], as previously described [11]. The size of the particles was estimated by non-denaturing gradient-gel electrophoresis [11] using the Pharmacia Phast System (Pharmacia Biotech). The phospholipid content of rHDL was determined by an enzymic method [20]. Proteins were measured by the method of Lowry et al. [21], using BSA as standard.

Electrophoretic procedures

DGGE across transverse urea gradients

Electrophoresis across transverse urea gradients [12,22] was carried out as previously described [14,23]. Four sample application trenches, 90 mm × 3 mm, 50 mm apart, were shaped in a 250 mm × 125 mm width-by-height mould (catalogue no. 80-1106-89 from Pharmacia). A denaturant gradient, 65 mm high and corresponding to 4.5 ml + 4.5 ml of solution, was cast between two 2-cm-high concentration plateaus. Urea was used at concentrations between 0 and 8 M. The running buffer was 43 mM imidazole/35 mM Hepes, pH 7.4 [24]. Polyacrylamide (PA) concentration in the slab was 5 % (total acrylamide content) and 4 % (ratio of cross-linker to total acrylamide monomer).

rHDL were dissolved in 10 mM phosphate buffer, pH 7.4, with or without 0.4 % NP40; 60 μl of sample solution was applied per lane. Gels were subjected to electrophoresis at 15 °C in a horizontal chamber (Multiphor II, Pharmacia), with an electrode distance of 22 cm and agarose strips as anolyte and catholyte. Electrophoretic runs were performed for 45 min at 400 V (see the Figure legends). Proteins were stained with 0.3 % Coomassie Brilliant Blue R-250 in ethanol/acetic acid/water (30:10:60, by vol.). For maximal resolution, delipidated apoA-I and A-I_M/A-I_M were run on a wider slab, cast with the no. 18-1013-74 (Pharmacia) cassette, as described in [19].

Qualitative and quantitative parameters have to be considered in the evaluation of a protein denaturation curve. Qualitative evaluation is based on pattern recognition. In the most typical situation, when urea concentration increases, a smooth change from higher to lower mobility is observed, yielding a sigmoidal curve. This behaviour implies a co-operative reversible transition between folded and unfolded conformation, with fast kinetics. Fast kinetics requires that, during the electrophoretic run, at least ten transitions occur between folded and unfolded state [13]. A sigmoidal curve may be quantitatively characterized by two parameters: (i) the urea concentration at one-half transition, $[U]_{0.5}$ [25], and (ii) the steepness of the curve in the transition region. The former parameter describes the overall stability of the protein against denaturation, whereas the latter describes the co-operativity of the transition and is believed to be proportional to the surface area that is buried in the native state but exposed to the denaturant agent in the unfolded state.

DGGE across transverse NP40 gradients

NP40 gradients, 0–0.1 %, were cast as described above, after addition of glycerol to the detergent-containing solution. Running conditions were as for urea DGGE gels.

DGGE across transverse SDS gradients

SDS gradients, 0–0.1 %, were cast as previously described [26]. Most features of the experimental set-up were similar to what has been detailed above for urea DGGE. The PA matrix varied between 5 % and 20 % total acrylamide, and 4 % bisacrylamide cross-linker. The anodic strip was agarose, while the cathodic

strip was PA, containing the same detergent gradient as in the resolving gel [26]. The field strength varied between 20 and 500 V/22 cm, and the duration of the experiments was from 1 to 10 h (see the Figure legends).

Data from SDS/DGGE runs in gels of varied total PA were analysed as described by Ferguson [27] for stepwise SDS concentrations (0–0.1 %). rHDL, whose hydrodynamic volumes had been assessed by gel filtration, were taken as references.

CD measurements

CD measurements were performed on a Jasco 500A spectropolarimeter, interfaced to a personal computer for data collection and manipulation. The spectra were analysed by means of the Jasco J700 software. The instrument was equipped with a thermostatically controlled cell holder (stabilized by circulating water from a bath); rectangular cuvettes with 0.1 cm path length were used. The instrument was calibrated with D-camphor-10-sulphonic acid solution. All spectra were baseline-corrected by subtracting buffer spectra. Protein concentration was 0.1 mg/ml, in Tris/HCl, pH 7.4. Samples were prepared by mixing a 1 mg/ml stock protein solution with urea powder and filling to the required volume; the final buffer concentration was 10 mM. Molar-mean-residue-ellipticity [θ] values were evaluated at 222 nm by the equation:

$$[\theta] = \theta_{obs} \cdot MWR/10dc$$

where θ_{obs} is the ellipticity measured in degrees, MWR is the mean residue molar weight of the examined protein, d is the optical path in centimetres and c is the protein concentration in g/ml. Data are expressed in terms of ratio between values measured at a given urea concentration and in the absence of urea.

RESULTS AND DISCUSSION

Urea/DGGE

Free apolipoproteins and detergent-treated rHDL

Purified apoA-I and dimeric A-I_M/A-I_M (1 mg/ml) were run across a transverse urea gradient from 0 to 4 M (Figure 1). For apoA-I (top panel), the pattern already described in [19] is observed, with a number of parallel tracings in the region between 1 and 3 M urea, over which the transition from folded (fast migrating) and unfolded (slow migrating) forms of the protein occurs. Size differences due to self-aggregation (isomerism) [10] have been reported to be the main cause of this peculiar multiple banding pattern [19]. For A-I_M/A-I_M (bottom panel), the transition begins just above 0 M urea and is completed around 2 M urea. As a further evidence of self-aggregation for both apolipoproteins, band width is much larger (3–4-fold) in the absence than in the presence of urea.

For monomeric apoA-I_M (reduced and reduced + alkylated), the unfolding transition begins at a slightly higher urea concentration than for dimeric A-I_M/A-I_M (Figure 2A). Over the transition region, the curve is steeper for the monomer than for the dimer. Under native conditions (in the absence of urea) the A-I_M/A-I_M dimer migrates about 50 % faster than monomeric apoA-I_M; in 8 M urea the mobility is very low and similar for monomer and dimer.Treating rHDL with non-ionic detergents is expected to strip apolipoproteins from lipids, while preventing their self-aggregation. When rHDL that contain apoA-I are added with 0.4 % (w/v) NP40, a typical sigmoidal pattern is observed in urea/DGGE, with an unfolding transition between

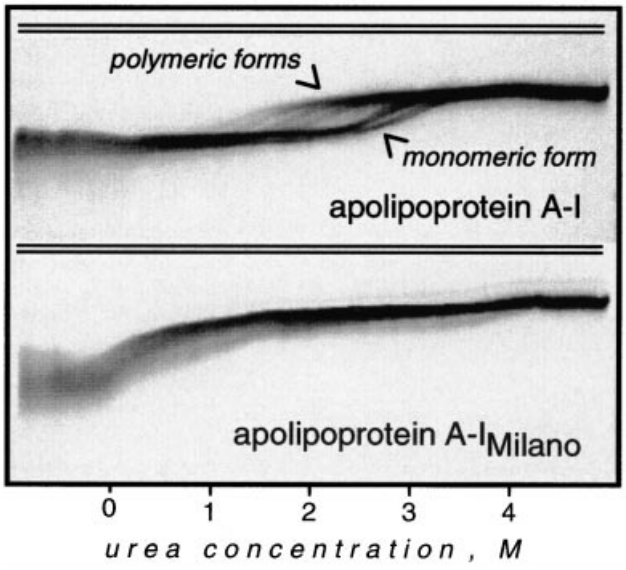

Figure 1 Urea/DGGE of apoA-I and A-I_M/A-I_M dimer over a 0–4 M urea concentration gradient

Sample application grooves are marked by a double line; the urea concentration increases from left to right (bottom scale); at the sides are two plateaux (without urea on the left; with 4 M urea on the right). Protein migration was towards the anode; the anode is at the bottom.

2 and 3 M urea (Figure 3). The absence of multiple banding in this experiment suggests that apoA-I is exclusively present in monomeric form. The single band observed in the transition region in Figure 3 corresponds to the most stable isomer noticed in Figure 1 for lipid-free apoA-I. A rather different pattern is observed for A-I_M/A-I_M rHDL. As in Figure 1, the shape of the curve is atypical, with a monotonous trend and the inflection point shifted close to the origin (0 M urea). In the transition region the denaturation curve of apoA-I is steeper than that of A-I_M/A-I_M.

The denaturation curves of apoA-I, dimeric A-I_M/A-I_M and monomeric apoA-I_M thus differ in several respects. A sigmoidal pattern in urea/DGGE, as observed for apoA-I and monomeric apoA-I_M, is the result of an exponential dependence upon urea concentration of the rate constants for unfolding and folding, k_U and k_N [12,13]. The urea concentration at one-half transition, $[U]_{0.5}$ [25], is < 2 M urea for dimeric A-I_M/A-I_M, 2.5 M urea for monomeric A-I_M and > 3 M urea for apoA-I; apolipoprotein stability against denaturation increases accordingly.

As implied by the different slopes of their denaturation curves in the transition region, the co-operativity in the unfolding process is lower for dimeric A-I_M/A-I_M than for apoA-I or for reduced (and reduced + alkylated) monomeric apoA-I_M. Moreover, for dimeric A-I_M/A-I_M, over the transition region, the curve is much steeper at lower than at higher urea concentration (Figures 1 and 3). Accordingly, intramolecular (protein–protein) interactions appear less uniform in dimeric A-I_M/A-I_M than in apoA-I and monomeric apoA-I_M; moreover, in the dimer, the unfolding process appears to be easier (more energetically favoured) at lower than at higher urea concentration. CD data confirm that, in A-I_M/A-I_M, some secondary structure is lost at very low urea concentration (Figure 4); the same occurs with guanidinium chloride (results not shown). This should involve a specific and unique structure, possibly in the region around the disulphide bridge and/or the monomer–monomer contact region.

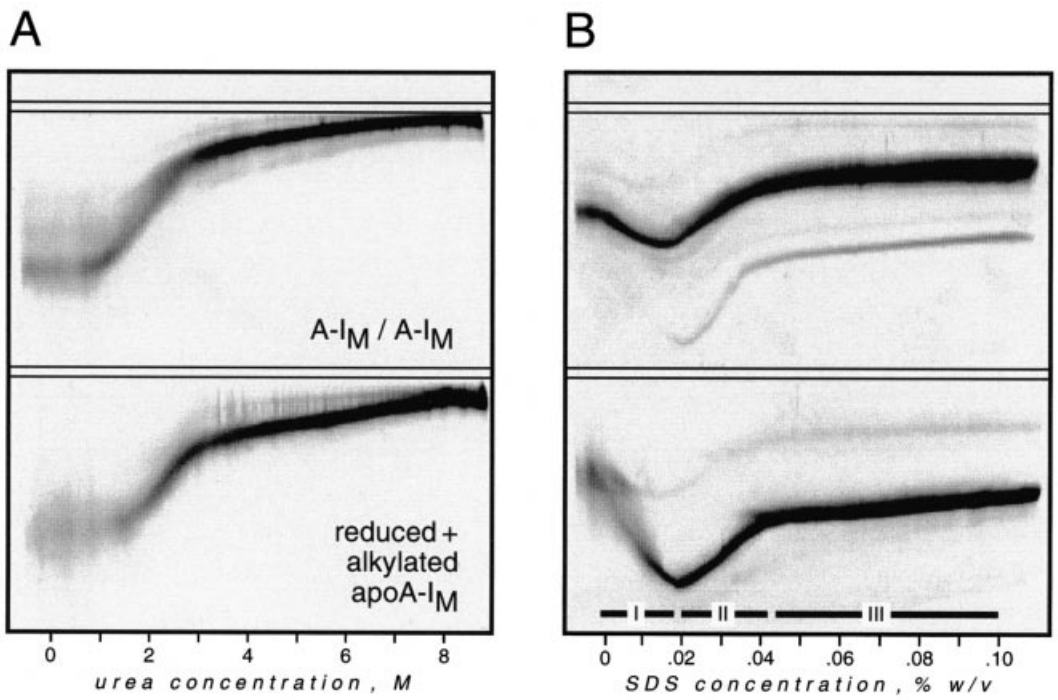

Figure 2 Urea/DGGE and SDS/DGGE for A-I$_M$/A-I$_M$ and for A-I$_M$

(**A**) Urea/DGGE over a 0–8 M urea concentration gradient for A-I$_M$/A-I$_M$ dimer (top) and for reduced alkylated A-I$_M$ (bottom). (**B**) SDS/DGGE over a 0–0.1 % concentration gradient for A-I$_M$/A-I$_M$ dimer (top) and for reduced alkylated A-I$_M$ (bottom).

rHDL

A contrasting behaviour is observed between small- and large-size rHDL: a single band is revealed for larger particles, two bands for smaller particles. The mobility of the bands (the faster one when split up) decreases continuously between 1 and 7 M urea (Figure 5).

The single curve for the larger particles (12.7 nm apoA-I rHDL/12.5 nm A-I$_M$/A-I$_M$ rHDL) has a different shape from the same rHDL added with NP40 (Figure 3); this observation implies that urea is not able to strip lipids away from larger-size rHDL. By contrast, for both smaller particles (7.8 nm apoA-I rHDL and 7.8 nm A-I$_M$/A-I$_M$ rHDL), at high urea concentration, a band with low mobility appears and its shape resembles that of the same rHDL treated with NP40 (Figure 3). For 7.8 nm apoA-I rHDL this band is faint between 4 M and 6 M urea, and only becomes strong above 6 M urea; for 7.8 nm A-I$_M$/A-I$_M$ rHDL the band is already detectable in approx. 1 M urea, to grow darker and darker at higher urea concentrations.

On the grounds of their identical behaviour, we conclude the species with low mobility observed in 8 M urea for small rHDL (Figure 5) are the same observed in rHDL pretreated with NP40 (Figure 3); they correspond to lipid-free apolipoprotein. This is consistent with increasing concentrations of urea being able to pull some apolipoprotein out of smaller rHDL with increasing efficiency.

The fast-migrating bands observed with smaller particles (7.8 nm apoA-I rHDL/7.8 nm A-I$_M$/A-I$_M$ rHDL) and the only component observed with larger particles (12.7 nm apoA-I rHDL/12.5 nm A-I$_M$/A-I$_M$ rHDL) (Figure 5) are then forms of lipid-bound protein. For the larger particles the change in mobility over the urea concentration gradient is minimal, hence the composition of the rHDL is hardly affected by the denaturing agent (loss of a small percentage of POPC, resulting in a slightly reduced charge density).

For 7.8 nm A-I$_M$/A-I$_M$ rHDL the hypothesis of a decreasing number of protein molecules per particle in the presence of increasing urea concentrations is untenable (A-I$_M$/A-I$_M$ rHDL$_{7.8\ nm}$ contains just one A-I$_M$/A-I$_M$ dimer); this conclusion may be extended by analogy to 7.8 nm apoA-I rHDL. It seems then that the large shift in mobility results from a progressive, non-co-operative loss of a large amount of bound POPC from small-size rHDL.

NP40/DGGE

rHDL

When rHDL are run across a transverse NP40 gradient, the shapes of the curves produced by the smaller particles (7.8 nm) are similar, irrespective of the apolipoprotein constituent (Figure 6). The shapes of the curves produced by the larger particles (12.7 and 12.5 nm) are also similar to one another, but different from the ones observed with smaller particles (Figure 6). In all instances, three sections may be recognized along the curves. In the first (I: below 0.01–0.02 % NP40), protein mobility decreases, with a greater shift for smaller than for larger rHDL; this feature results from progressive loss (delipidation) of the charged POPC from rHDL. Conversely, mobility is constant across the last section of the curve (III: above 0.05 % NP40); the migrating species correspond to lipid-stripped detergent-laden apolipoproteins, with a defined and stable structure. In the intermediate section (II), the blurred protein bands are a result of a minor decrease in mobility; essentially lipid-free, misfolded apolipo-

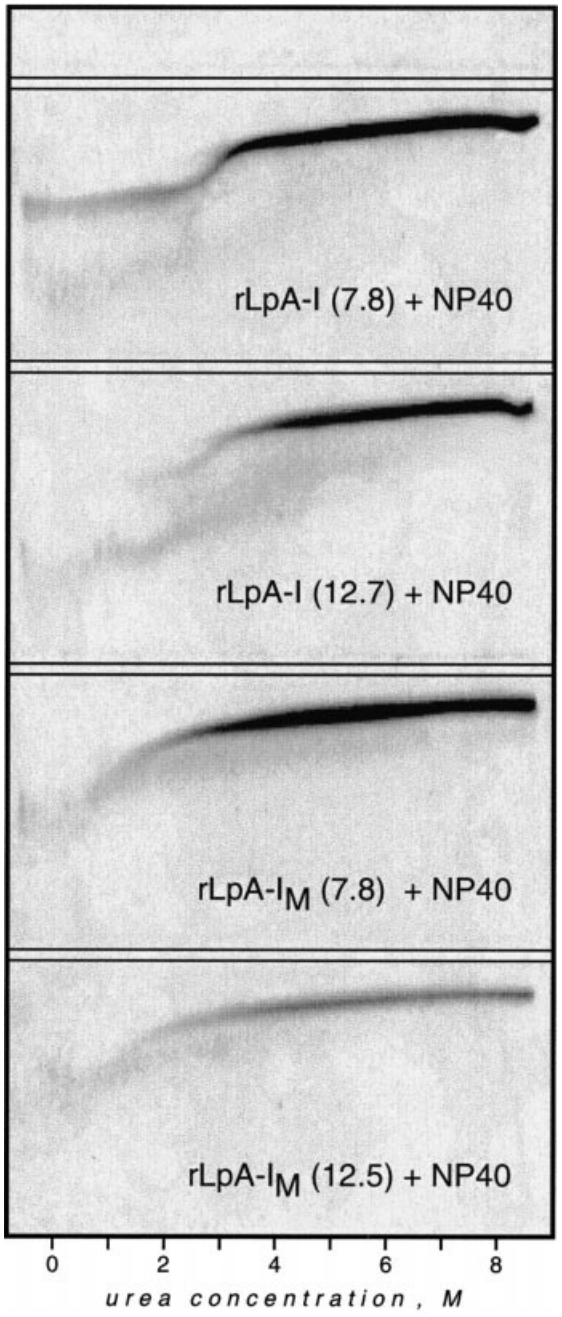

Figure 3 Urea/DGGE over a 0–8 M urea concentration gradient of rHDL added with 0.4% NP40

Samples, from top to bottom: 7.8 nm apoA-I rHDL, 12.7 nm apoA-I rHDL, 7.8 nm A-I$_M$/A-I$_M$ rHDL,12.5 nm A-I$_M$/A-I$_M$ rHDL. All samples migrated at the same time in a single gel, from four parallel grooves. The anode is at the bottom; electrophoresis was run for 45 min at 400 V/22 cm.

proteins should be present in this detergent concentration range. Except for 7.8 nm A-I$_M$/A-I$_M$ rHDL, all curves display a discontinuity between the first and the second of the above sections, which implies that some steps along the pathway from lipid-bound to lipid-free protein are so slow (less than ten transitions in 60 min) as to be undetectable under our experimental conditions. In contrast, the interconversion between misfolded and properly folded conformation of the lipid-stripped

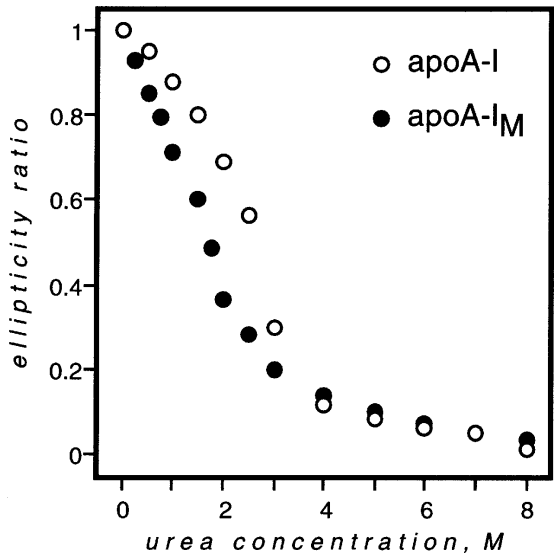

Figure 4 CD of apoA-I and apoA-I$_M$ in the presence of urea

Ellipticity was evaluated at 222 nm; data are expressed in terms of the ratio between values measured at a given urea concentration and in the absence of urea.

apolipoproteins appears fast under the detailed experimental conditions, as no discontinuity is observed between the second and the third section of the curves.

The mobilities of stripped, unfolded apoA-I and dimeric A-I$_M$/A-I$_M$ are very similar to one another (refer to the 8 M urea plateau in Figures 3 and 5), whereas the mobility of lipid-stripped, detergent-laden monomeric A-I (above approx. 0.05% detergent) is almost twice as high as that of dimeric A-I$_M$/A-I$_M$ (NP40 plateau in Figure 6). Accordingly, in 8 M urea, a completely stretched, unfolded structure is assumed. The hydrodynamic volume appears to depend entirely on the major radius, so apoA-I and dimeric A-I$_M$/A-I$_M$ have probably identical length and similar behaviour. In contrast, after lipid stripping and binding of non-ionic detergent, the diameter of dimeric A-I$_M$/A-I$_M$ is approx. twice as large as for monomeric apoA-I.

SDS/DGGE

Monomeric apoA-I$_M$

Monomeric apoA-I$_M$ and dimeric A-I$_M$/A-I$_M$ bind SDS with a different pattern (Figure 2B). In both cases the protein mobility increases at first, and then decreases. For dimeric A-I$_M$/A-I$_M$ maximal mobility is attained around 0.013% SDS, and for monomeric apoA-I$_M$ around 0.020%. The increase in mobility is much higher for monomeric apoA-I$_M$ than for dimeric A-I$_M$/A-I$_M$ (about 3-fold). Plateauing is for both around 0.04% SDS. Mobility of the SDS-saturated species is lower than mobility of ligand-free species for dimeric A-I$_M$/A-I$_M$ and higher for monomeric apoA-I$_M$.

rHDL

Three sections may be recognized in SDS/DGGE curves (Figure 7). The first, below 0.01% SDS, corresponds to intact, unaffected particles. The width of this plateau is similar for all four test particles. The last section, characterized by constant protein mobility, corresponds to lipid-stripped SDS-laden apolipopro-

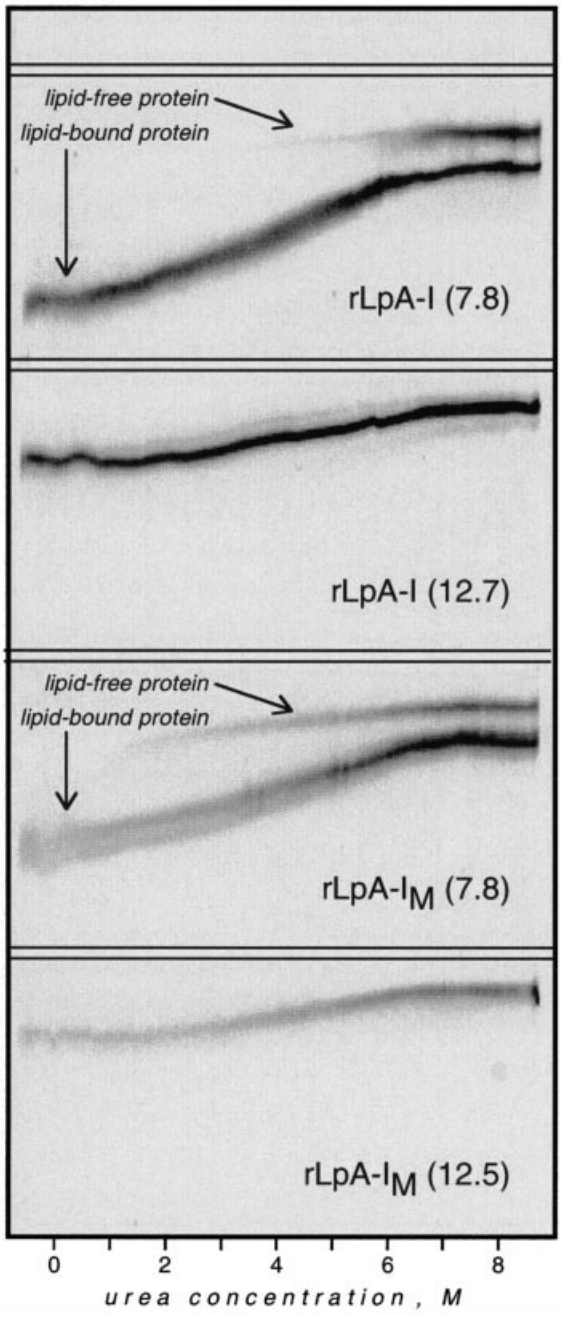

Figure 5 Urea/DGGE of rHDL over a 0–8 M urea concentration gradient

Electrophoresis was run for 45 min at 400 V/22 cm. The samples were as in Figure 3.

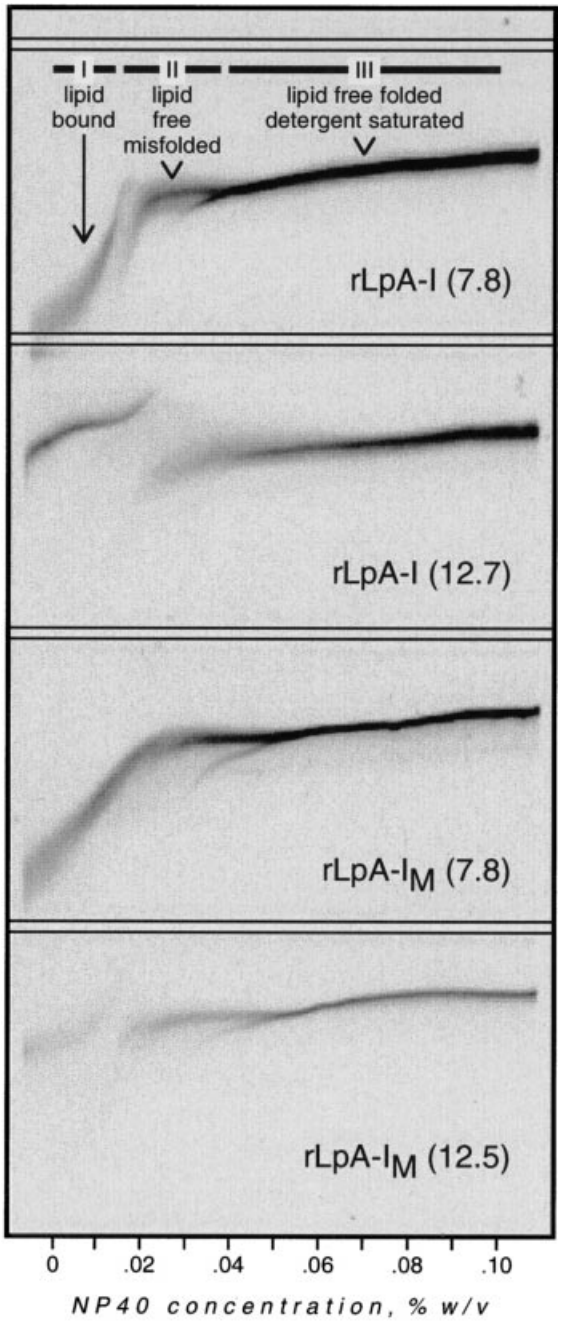

Figure 6 NP40/DGGE of rHDL over a 0–0.1% concentration gradient of the detergent

Electrophoresis was run for 60 min at 400 V/22 cm. Samples were as in Figure 3.

teins. This situation is attained around 0.03 % SDS for apolipoproteins from smaller particles, 7.8 nm apoA-I rHDL/7.8 nm A-I$_M$/A-I$_M$ rHDL, versus about 0.04 % SDS for larger particles, 12.7 nm apoA-I rHDL/12.5 nm A-I$_M$/A-I$_M$ rHDL. Delipidation, SDS binding and protein unfolding should then occur in the intermediate region. For apolipoproteins deriving from smaller rHDL, a decrease in mobility is observed before plateauing; by contrast, an increase in the same region can be detected for apolipoproteins deriving from larger rHDL. In 7.8 nm particles the last process to go to completion appears thus to be increase in volume, with concurrent decrease in charge density. For larger particles a readily reversible increase in charge is observed over the SDS concentration range 0.025–0.035 %. SDS–DGGE runs during 1 or 10 h under varying electric fields to total identical V · h result in essentially identical patterns (not shown); all the kinetic constants (un-/re-folding, lipid/detergent binding), in experiments showing discontinuous transition, are slower than 10 h.

The features of the denaturation curves of rHDL in SDS/DGGE appear to depend markedly upon the PA concentration of the running gel. This is especially true for SDS concentrations lower than 0.07 %.

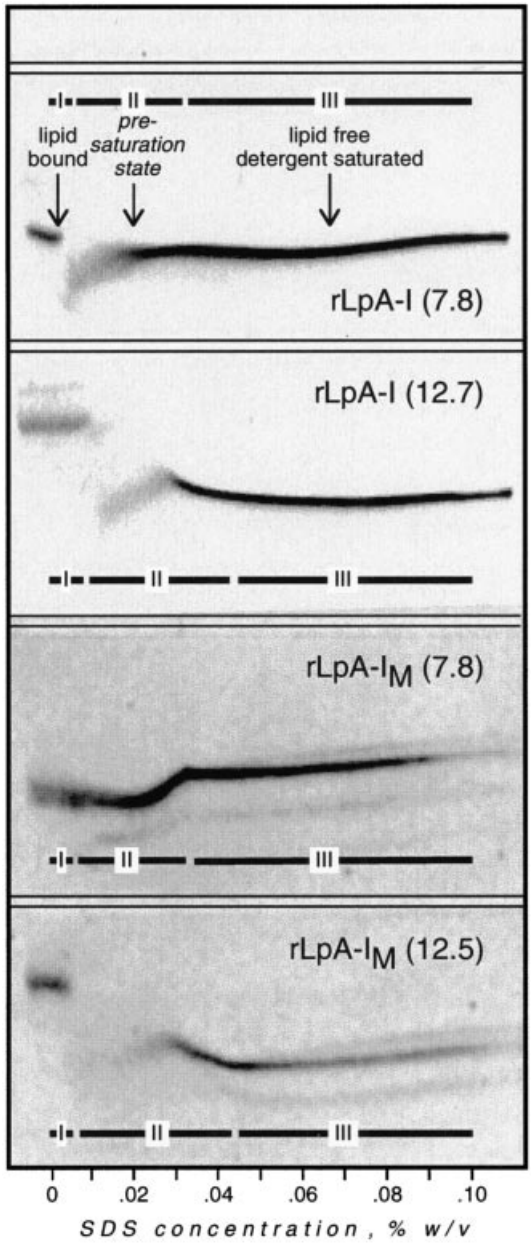

Figure 7 SDS/DGGE of rHDL over a 0–0.1% concentration gradient of the detergent

Electrophoresis was run for 60 min at 200 V/22 cm, in a 5% total acrylamide gel. Samples were as in Figure 3.

This aspect was investigated in detail for 7.8 nm apoA-I rHDL. While in 5% total acrylamide a sharp band is observed, which implies no differential sieving by the gel matrix on the migrating components, a blurred and very wide band is seen at higher PA concentrations, to become again a sharp band with a fuzzy front at the highest PA concentration investigated (20% total acrylamide) (Figure 8A). By data reduction according to Ferguson [27], the K_r (retardation coefficient) of the faster and slower fronts of the protein band can be computed. According to Ferguson, K_r depends solely on particle size, and this parameter can be useful to analyse delipidation of rHDL versus unfolding of apoprotein components. In Figure 8(B), K_r values calculated at different SDS concentrations are reported. They reflect a very heterogeneous behaviour for rHDL. Delipidation of rHDL, with volume reduction, and denaturation of apoA-I, with volume expansion, can occur at similar or at different SDS concentration. Fast front is shaped by rHDL in which lipid-stripping (at low detergent concentration) and protein denaturation (at high detergent concentration) appear to occur at different SDS concentrations. Slow front, on the contrary, corresponds to rHDL in which the two phenomena occur at once all along the SDS concentration range (Figure 8B).

From runs across the SDS gradient in a 5%-total-acrylamide gel (Figure 7), rHDL structure appears affected by even the lowest amounts of SDS, while constant mobility is attained at SDS concentrations $\geqslant 0.04\%$.

An underlying complexity of the phenomena in the pre-saturation state, i.e. over the SDS concentration range 0–0.4%, is made evident by multiple runs in gels of increasing total percentage acrylamide according to Ferguson [27]. For apoA-I (7.8 nm rHDL), a large heterogeneity in size of the particles is demonstrated at intermediate SDS concentrations (Figure 8). Changes in size are not monotonous, which may result from a shifting equilibrium between the denaturation of the apoprotein component and the removal of POPC molecules.

For this experiment seven gels were run, with total percentage acrylamide between 5 and 20. Calculations, however, were performed on data from 5 to 15% total acrylamide runs only, disregarding migration distances < 5 mm. This limitation had to be excepted for the 12.7 nm rHDL, whose migration already decreased to 1 mm in 10% total acrylamide. The K_r of the latter was thus affected by higher uncertainty, which is why the second-pass calculations made as described by Ferguson, i.e. transformation of K_r into size, are not reported.

CONCLUSIONS

The present investigation by electrophoretic techniques of the dissociation–denaturation behaviour of small and large rHDL containing two forms of apoA-I, which differ sharply in secondary and tertiary structure, clearly demonstrates that particle size is the major determinant of rHDL stability. The large rHDL containing either apoA-I, or the dimeric A-I$_M$/A-I$_M$, are far more stable than the corresponding smaller particles. Indeed, a remarkable and similar amount of both apolipoproteins is stripped free of lipids from small rHDL, whereas no apolipoprotein dissociation is observed with the large rHDL. The higher stability of large rHDL likely reflects a higher number of protein–lipid and lipid–lipid interactions in large compared with small rHDL. Indeed, the large particles lose some of the bound phospholipids while still maintaining their properties of protein–lipid complexes, whereas the small particles, once the little phospholipid they contain is lost, release a significant amount of the bound protein.

Early spectroscopic studies on apoA-I-containing discoidal rHDL showed a progressive increase in rHDL stability as particle diameter increases from 9.3 to 18.6 nm [28,29]. In the present studies we used two sets of small and large rHDL of similar size, which contain either apoA-I, or the disulphide-linked A-I$_M$/A-I$_M$ dimer, to investigate whether protein structure/composition may affect the size-dependent stability of rHDL particles. Previous spectroscopic and limited proteolysis studies have established that the two proteins adopt different conformations when incorporated into same-sized rHDL [11,30]. The present data thus demonstrate that particle size is a stronger determinant of rHDL stability than protein structure/conformation.

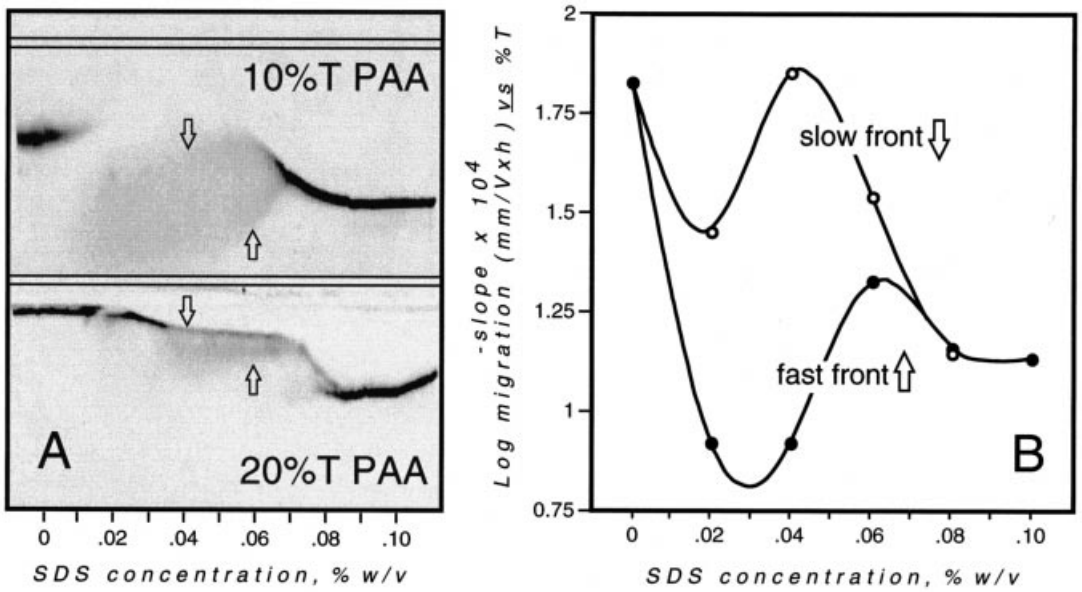

Figure 8 Ferguson plot of apoA-I migration in the presence of SDS

(**A**) SDS/DGGE over a 0–0.1% concentration gradient of the detergent, for 7.8 nm apoA-I rHDL. Top: in a 10%-total-acrylamide gel ('10%T PAA'); electrophoresis was run for 90 min at 400 V/22 cm. Bottom: in a 20%-total-acrylamide gel ('20%T PAA'); electrophoresis was run for 10 h at 500 V/22 cm. (**B**) Reduction, as described by Ferguson [27], of data from SDS/DGGE (in **A**), for slow and fast front of the band from 7.8 nm apoA-I rHDL. Left axis: first-pass calculation; K_r as a function of SDS concentration.

This finding may have physiological implications for the major functions of HDL, i.e. the ability to promote cholesterol efflux from peripheral cells and the subsequent transport to the liver for excretion. Cholesterol efflux to extracellular acceptors occurs through two distinct pathways [31]: (i) interaction between lipid-free apoA-I and a specific site on the cell surface, with membrane micro-solubilization and generation of small lipid-poor HDL; and (ii) a relatively non-specific interaction of phospholipid-containing acceptors, including lipid-poor HDL, with the cell, and diffusion of cholesterol from the cell membrane into the lipoprotein surface. The first pathway appears to be mediated by the ABCA1 transporter [32], the second by the membrane protein SR-BI [33]. The low stability of the small rHDL, which mimic the lipid-poor HDL generated through the interaction of lipid-free apoA-I with the ABCA1 transporter, indicates that these are relatively unstable structures that can undergo either stabilization or destabilization, through distinct pathways. They may further interact with cell membranes, in an attempt to stabilize their structure by acquiring additional lipid molecules through SR-BI, or may deliver lipids to large, stable HDL that serve as cholesterol sinks [34], with release of lipid-free apolipoprotein that recycles as phospholipid and cholesterol acceptor.

This work was supported in part by a grant from the Ministero dell'Università e della Ricerca Scientifica (MURST) (COFIN 2000–2001: Structural studies on hydrophobic molecule-binding proteins) to E.G. and I.E.

REFERENCES

1 Narayanaswami, V. and Ryan, R. O. (2000) Molecular basis of exchangeable apolipoprotein function. Biochim. Biophys. Acta **1483**, 15–36
2 Nolte, R. T. and Atkinson, D. (1992) Conformational analysis of apolipoprotein A-I and E-3 based on primary sequence and circular dichroism. Biophys. J. **63**, 1221–1239
3 Segrest, J. P., Jones, M. K., De Loof, H., Brouillette, C. G., Venkatachalapathi, Y. V. and Anantharamaiah, G. M. (1992) The amphipathic helix in the exchangeable apolipoproteins: a review of secondary structure and function. J. Lipid Res. **31**, 141–166
4 Phillips, J. C., Wriggers, W., Li, Z., Jonas, A. and Schulten, K. (1997) Predicting the structure of apolipoprotein A-I in reconstituted high-density lipoprotein disks. Biophys. J. **73**, 2337–2346
5 Segrest, J. P., Jones, M. K., Klon, A. E., Sheldahl, C. J., Hellinger, M., De Loof, H. and Harvey, S. C. (1999) A detailed molecular belt model for apolipoprotein A-I in discoidal high density lipoprotein. J. Biol. Chem. **274**, 31755–31758
6 Tricerri, M. A., Behling Agree, A. K., Sanchez, S. A., Bronski, J. and Jonas, A. (2001) Arrangement of apolipoprotein A-I in reconstituted high-density lipoprotein disks: an alternative model based on fluorescence resonance energy transfer experiments. Biochemistry **40**, 5065–5074
7 Jonas, A. (1986) Reconstitution of high-density lipoproteins. Methods Enzymol. **128**, 553–582
8 Weisgraber, K. H., Rall, Jr., S. C., Bersot, T. P., Mahley, R. W., Franceschini, G. and Sirtori, C. R. (1983) Apolipoprotein AI_{Milano}: detection of normal AI in affected subjects and evidence for a cysteine for arginine substitution in the variant AI. J. Biol. Chem. **258**, 2508–2513
9 Franceschini, G., Vecchio, G., Gianfranceschi, G., Magani, D. and Sirtori, C. R. (1985) Apolipoprotein $A\text{-}I_{Milano}$: accelerated binding and dissociation from lipids of a human apolipoprotein variant. J. Biol. Chem. **260**, 16321–16325
10 Calabresi, L., Vecchio, G., Longhi, R., Gianazza, E., Palm, G., Wadensten, H., Hammarström, A., Olsson, A., Karlström, A., Sejlitz, T. et al. (1994) Molecular characterization of native and recombinant apolipoprotein $A\text{-}I_{Milano}$ dimer: the introduction of an interchain disulfide bridge remarkably alters the physicochemical properties of apolipoprotein A-I. J. Biol. Chem. **269**, 32168–32174
11 Calabresi, L., Vecchio, G., Frigerio, F., Vavassori, L., Sirtori, C. R. and Franceschini, G. (1997) Reconstituted high-density lipoproteins with a disulfide-linked apolipoprotein A-I dimer: evidence for restricted particle size heterogeneity. Biochemistry **36**, 12428–12433
12 Creighton, T. E. (1979) Electrophoretic analysis of the unfolding of proteins by urea. J. Mol. Biol. **129**, 235–264
13 Creighton, T. E. (1980) Kinetic study of protein unfolding and refolding using urea gradient electrophoresis. J. Mol. Biol. **137**, 61–80
14 Gianazza, E., Eberini, I., Santi, O. and Vignati, M. (1998) Denaturant-gradient gel electrophoresis: technical aspects and practical applications. Anal. Chim. Acta **372**, 99–120

15 Evans, R. W. and Williams, J. (1980) The electrophoresis of transferrins in urea/polyacrylamide gels. Biochem. J. **189**, 541–546
16 Yamashita, H., Nakatsuka, T. and Hirose, M. (1995) Structural and functional characteristics of partially disulfide-reduced intermediates of ovotransferrin N lobe: cystine localization by indirect end-labeling approach and implications for the reduction pathway. J. Biol. Chem. **270**, 29806–29812
17 Ewbank, J. J. and Creighton, T. E. (1993) Structural characterization of the disulfide folding intermediates of bovine α-lactalbumin. Biochemistry **32**, 3694–3707
18 Gianazza, E., Sirtori, C. R., Castiglioni, S., Eberini, I., Chrambach, A., Rondanini, A. and Vecchio, G. (2000) Interactions between carbonic anhydrase and its inhibitors revealed by gel electrophoresis and circular dichroism. Electrophoresis **21**, 1435–1445
19 Gianazza, E., Calabresi, L., Santi, O., Sirtori, C. R. and Franceschini, G. (1997) Denaturation and self-association of apolipoprotein A-I investigated by electrophoretic techniques. Biochemistry **36**, 7898–7905
20 Takayama, M., Itoh, S., Nagasaki, T. and Tanimizu, I. (1977) A new enzymatic method for determination of serum choline-containing phospholipids. Clin. Chim. Acta **79**, 93–96
21 Lowry, O. H., Rosebrough, N. J., Farr, A. L. and Randall, R. J. (1951) Protein measurement with the Folin phenol reagent. J. Biol. Chem. **193**, 265–275
22 Creighton, T. E. (1986) Detection of folding intermediates using urea-gradient electrophoresis. Methods Enzymol. **131**, 156–172
23 Gianazza, E., Galliano, M. and Miller, I. (1997) Structural transitions of human serum albumin: an investigation using electrophoretic techniques. Electrophoresis **18**, 695–700
24 Goldenberg, D. P. (1989) Analysis of protein conformation by gel electrophoresis. In Protein Structure: a Practical Approach (Creighton, T. E., ed.), pp. 225–250, IRL Press, Oxford
25 Masson, P. and Goasdoue, J. L. (1986) Evidence that the conformational stability of 'aged' organophosphate-inhibited cholinesterase is altered. Biochim. Biophys. Acta **869**, 304–313
26 Gianazza, E., Vignati, M., Santi, O. and Vecchio, G. (1998) Electrophoresis of proteins across a transverse sodium dodecyl sulfate gradient. Electrophoresis **19**, 1631–1641
27 Ferguson, K. A. (1964) Starch-gel electrophoresis: application to the classification of pituitary proteins and polypeptides. Metab. Clin. Exp. **13**, 985–992
28 Sparks, D. L., Lund-Katz, S. and Phillips, M. C. (1992) The charge and structural stability of apolipoprotein A-I in discoidal and spherical recombinant high density lipoprotein particles. J. Biol. Chem. **267**, 25839–25847
29 Wald, J. H., Krul, E. S. and Jonas, A. (1990) Structure of apolipoprotein A-I in three homogeneous, reconstituted high density lipoprotein particles. J. Biol. Chem. **265**, 20037–20043
30 Calabresi, L., Tedeschi, G., Treu, C., Ronchi, S., Galbiati, D., Airoldi, S., Sirtori, C. R., Marcel, Y. and Franceschini, G. (2001) Limited proteolysis of a disulfide-linked apoA-I dimer in reconstituted HDL. J. Lipid Res. **42**, 935–942
31 Yokoyama, S. (2000) Release of cellular cholesterol: molecular mechanism for cholesterol homeostasis in cells and in the body. Biochim. Biophys. Acta **1529**, 231–244
32 Attie, A. D., Kastelein, J. P. and Hayden, M. R. (2001) Pivotal role of ABCA1 in reverse cholesterol transport influencing HDL levels and susceptibility to atherosclerosis. J. Lipid Res. **42**, 1717–1726
33 Ji, Y., Jian, B., Wang, N., Sun, Y., Moya, M. L., Phillips, M. C., Rothblat, G. H., Swaney, J. B. and Tall, A. R. (1997) Scavenger receptor BI promotes high density lipoprotein-mediated cellular cholesterol efflux. J. Biol. Chem. **272**, 20982–20985
34 Rothblat, G. H., de la Llera-Moya, M., Atger, V., Kellner-Weibel, G., Williams, D. L. and Phillips, M. C. (1999) Cell cholesterol efflux: integration of old and new observations provides new insights. J. Lipid Res. **40**, 781–796

Received 9 January 2002/30 April 2002; accepted 8 May 2002
Published as BJ Immediate Publication 8 May 2002, DOI 10.1042/BJ20020058